

# Monolayer Adsorption Behavior of Hydrogen Isotopes on Microporous and Mesoporous Molecular Sieves

Xiao-Zhong Chu,\* Ji-Ming Xu, Yi-Jiang Zhao, Wei-Guang Zhang, Zhi-Peng Chen, and Shou-Yong Zhou

Jiangsu Key Laboratory for Chemistry of Low-Dimensional Materials, School of Chemistry and Chemical Engineering, Huaiyin Normal University, Huaian, 223300, P. R. China

Ya-Ping Zhou and Li Zhou

High Pressure Adsorption Laboratory, State Key Laboratory of Chemical Engineering, Tianjin University, Tianjin, 300072, P. R. China

The equilibrium adsorption amounts of hydrogen isotope gas and the Brunauer–Emmett–Teller (BET) surface area were measured at 77 K with different microporous and mesoporous molecular sieves. The results indicate that good linear relationships are observed between the amount adsorbed and the BET surface area at (0.02, 0.04, 0.06, 0.08, 0.10, and 0.12) MPa for microporous or mesoporous adsorbents, which provide proof of the monolayer adsorption mechanism for hydrogen isotopes at supercritical temperatures. Effects of specific surface area and pore size are more important than the surface properties of adsorbents for hydrogen isotope storage with the physical adsorption method. The equilibrium adsorption difference between hydrogen and deuterium is increased with a decrease of pressure. Moreover, the adsorption capacity of hydrogen isotopes on mesoporous molecular sieves is smaller than that on microporous molecular sieves at the same temperature, pressure, and BET surface area.

## Introduction

Hydrogen is a desirable energy source because it is renewable and its use would reduce emission pollution. The heavy isotope of hydrogen, deuterium, is an important material in the nuclear industry. It also has important applications in medical cures and as a tracer. Thus, the search for a suitable storage or separation carrier of hydrogen isotope gas continues to be a high priority. This problem receives research interest again following the increasing attention paid to green alternative energy and nuclear energy. Carriers of storage or separation which have been studied the most are activated carbon,<sup>1</sup> carbon nanotubes,<sup>2</sup> metal hydride,<sup>3</sup> and so forth, and it was concluded the storage capacity only depends on the specific surface area of adsorbents if the interaction between the hydrogen and the solid surface remains the van der Waals force.<sup>4,5</sup> However, this adsorption behavior for hydrogen isotope gas has not been investigated systematically on microporous and mesoporous molecular sieves.

In this study, for the purpose of further investigations on the monolayer mechanism of physical adsorption, the measurements for adsorption behavior of hydrogen isotopes were carried out on microporous and mesoporous molecular sieves, to explore if it is suitable to apply molecular sieves as adsorbents to hydrogen isotope gas storage or separation.

## Experimental Section

**Materials and Instruments.** The zeolites 3A, 4A, ZSM-5, and Pd-4A were provided by Heng-Ye Molecular Sieves, Ltd., Shanghai, CMS and the zeolites 5A, VP800-5, and 10X were provided by Jing-Zhong Molecular Sieves, Ltd., Shanghai. Y

zeolite was provided by the Molecular Sieve Factory, Nankai University, Tianjin. Mesoporous molecular sieves SBA-15 and CMK-3 were synthesized in the authors' laboratory. SBA-15 silica with two-dimensional ordered channels was synthesized in acidic conditions, and a nonionic oligomeric alkyethylene oxide surfactant (Pluronic P123) was used as the structure-directing agent; TEOS (tetraethyl orthosilicate) of analysis grade was used as the silica source. The carbon replica CMK-3 was synthesized using SBA-15 as the template and sucrose as the carbon source. Details of the synthesis were reported by us previously.<sup>6–8</sup> Additionally, adsorbents of SBA-15(a to d) were modified with different CuCl loading. The experimental process was as follows: First, the prepared mixture was heated from room temperature to 200 °C at the rate of 2 °C/min and kept there for 2 h. Secondly, it was heated to 350 °C at the same rate and kept there for 2 h. Finally, it is cooled to room temperature.<sup>9</sup> The three operation processes above were conducted in a nitrogen atmosphere. All adsorbents were dried in a vacuum at 150 °C for 24 h before the adsorption measurements.

Hydrogen of purity above 99.995 % was provided by the Liu-Fang High-Tech Co., China. Deuterium of purity above 99.9 % was provided by the Haipu Gas Industry Co., Beijing. An AS-3100Plus specific surface area and pore size analyzer was provided by Beckman Coulter, USA. The pressure transducer and molecular pump were provided by Pfeifer Vacuum, Germany, and the pressure sensor has a precision of 0.2 %. The rotary pump was provided by the Vacuum Pump Co., Wuxi.

**Apparatus and Procedure.** It is impossible to use a microbalance at 77 K; therefore, the equilibrium adsorption data were collected with the volumetric setup in Figure 1 that was commonly used for the adsorption of nitrogen at 77 K to evaluate the Brunauer–Emmett–Teller (BET) surface area of adsorbents. The adsorption cell is initially in vacuum (0.01 Pa)

\* Corresponding author. E-mail: chuxiaozhong@hytc.edu.cn. Tel.: (86)0517-83050008. Fax: (86)0517-83525369.

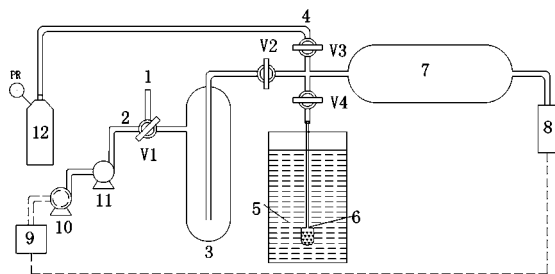


**Figure 1.** Schematic apparatus for adsorption experiments: 1, vent; 2, vacuum exit; 3, buffer bottle; 4, feed gas inlet; 5, liquid tank; 6, adsorption cell; 7, reference cell; 8, pressure transmitter; 9, online data recorder system; 10, molecular pump; 11, vacuum pump; V1, three-way vacuum valve; V2, V3, V4, two-way vacuum valve.

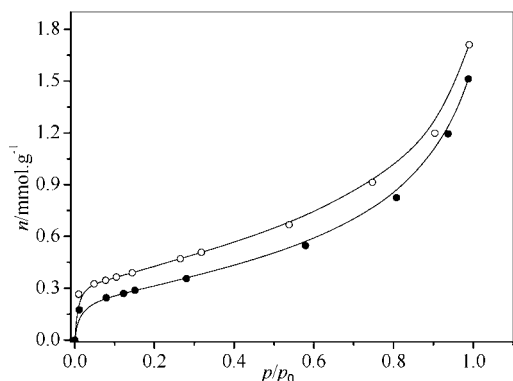


**Figure 2.**  $N_2$  adsorption isotherms at 77 K on 3A and Pd-4A.  $\circ$ , 3A;  $\bullet$ , Pd-4A.

for the equilibrium adsorption measurements. However, the pressure in the adsorption cell was increased stepwise up to 0.12 MPa for collecting equilibrium isotherms. The temperature of the reference cell was kept constant within  $\pm 0.2$  K, and the temperature of the adsorption cell was kept constant at 77 K with liquid nitrogen at a constant level. The absolute relative error calculated for the adsorption amount was within 2.0.<sup>10</sup>

## Results and Discussion

**1.  $N_2$  Adsorption Isotherms.** At present, there are many ways to obtain the specific surface area of different microporous materials, such as the BET method, the t-method, the  $\alpha_s$ -method, and the Dubinin–Radushkevich (DR) method, and so forth. The merits and limitations of these different methods were discussed in detail.<sup>11,12</sup> As is known, no method can determine the exact value of specific surface area for different microporous adsorbents. However, the BET method remains the most used in spite of some disadvantages in the theoretical aspect.<sup>11,13,14</sup> Therefore, to obtain comparable values of the specific surface area for different microporous and mesoporous molecular sieves, we measured the specific surface area with the BET method. Nitrogen adsorption isotherms of all adsorbents were measured at 77 K with the volumetric method. Obviously, 3A and Pd-4A are microporous materials, although their nitrogen adsorption curves in Figure 2 are type II isotherms according to the International Union of Pure and Applied Chemistry (IUPAC) classification.<sup>15,16</sup> The reason is that nitrogen molecules cannot diffuse into their pores at 77 K; therefore, the contribution to the BET surface area is mainly from the external surface of the adsorbents. It can be found from Figure 3 that the nitrogen adsorption curves of 4A, 5A, VP800-5, Y, 10X, CMS, and 13X are of type I that are typical for microporous adsorbents. As shown in Figure 4, the main characteristic feature of the nitrogen

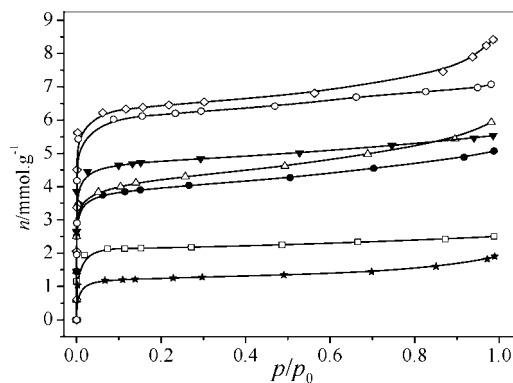


**Figure 3.**  $N_2$  adsorption isotherms at 77 K on different microporous molecular sieves.  $\diamond$ , 10X;  $\circ$ , VP800-5;  $\nabla$ , Y;  $\triangle$ , CMS;  $\bullet$ , 5A;  $\square$ , 4A;  $\star$ , 13X.

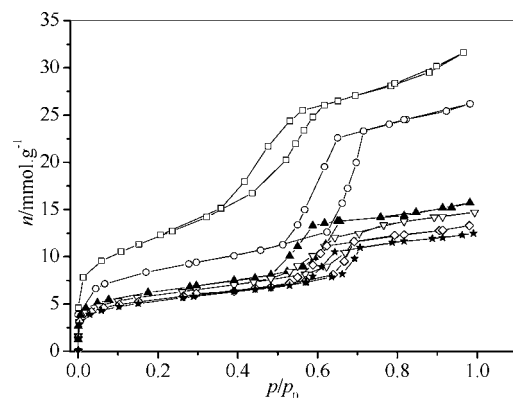


**Figure 4.**  $N_2$  adsorption isotherms at 77 K on different mesoporous molecular sieves.  $\square$ , CMK-3;  $\circ$ , SBA-15;  $\blacktriangle$ , SBA-15 (a);  $\nabla$ , SBA-15 (b);  $\diamond$ , SBA-15 (c);  $\star$ , SBA-15 (d).

adsorption–desorption curves for CMK-3 and SBA-15 is a hysteresis loop that is associated with mesoporosity and capillary condensation.<sup>15,16</sup> The modified SBA-15 molecular sieves still keep the mesoporous structure that are demonstrated by X-ray diffraction (XRD), scanning electron microscopy (SEM), transmission electron microscopy (TEM), and X-ray photoelectron spectroscopy (XPS) analysis in the previous paper.<sup>17</sup> Moreover, the results are also confirmed with the nitrogen adsorption–desorption isotherms in Figure 4. The BET surface areas of all adsorbents are listed in Table 1, based on the BET theory.<sup>15</sup>

**2.  $H_2$  and  $D_2$  Adsorption Isotherms.** Hydrogen and deuterium adsorption isotherms at 77 K were collected with the experimental apparatus in Figure 1, and the results are shown in Figures 5 to 9. On the basis of these adsorption isotherms, the amounts adsorbed at (0.02, 0.04, 0.06, 0.08, 0.10, and 0.12) MPa were obtained and listed in Table 1. The results indicate that a little difference is observed between  $H_2$  and  $D_2$  in each section and the amount adsorbed of  $D_2$  on different adsorbents is larger than that of  $H_2$ . It tells us that the deuterium molecules are preferentially adsorbed on these adsorbents. This fact is important for the pressure swing adsorption (PSA) technology because it determines which isotope is the column top product.<sup>18</sup> In addition, the equilibrium adsorption difference between hydrogen and deuterium is increased with a decrease of pressure according to the ratio of the amount adsorbed of  $D_2$  over  $H_2$  ( $R_{D/H}$ ) in Table 1; therefore, a suitable low pressure should be selected when the gas separation of a hydrogen isotope mixture is carried out.

**3. Relationship between Amount Adsorbed and BET Surface Area.** As shown in Figures 10 to 12, the amount adsorbed at (0.02, 0.06, and 0.12) MPa are plotted against the

**Table 1. BET Surface Area, Amount Adsorbed, and Ratio of Adsorption Amount at Different Pressures on Molecular Sieves**

molecular sieves	$S_{\text{BET}}$ $\text{m}^2 \cdot \text{g}^{-1}$	0.02 MPa			0.04 MPa			0.06 MPa			0.08 MPa			0.10 MPa			0.12 MPa		
		$\text{H}_2$	$\text{D}_2$	$R_{\text{D/H}}$	$\text{H}_2$	$\text{D}_2$	$R_{\text{D/H}}$	$\text{H}_2$	$\text{D}_2$	$R_{\text{D/H}}$	$\text{H}_2$	$\text{D}_2$	$R_{\text{D/H}}$	$\text{H}_2$	$\text{D}_2$	$R_{\text{D/H}}$	$\text{H}_2$	$\text{D}_2$	$R_{\text{D/H}}$
3A	33.00	0.04583	0.05173	1.13	0.07179	0.07836	1.09	0.09079	0.09604	1.06	0.1064	0.1117	1.05	0.1202	0.1251	1.04	0.1315	0.1367	1.04
4A	168.58	1.0923	1.2291	1.13	1.4024	1.5210	1.08	1.5848	1.7000	1.07	1.7034	1.7946	1.05	1.7988	1.8900	1.05	1.8683	1.9686	1.05
5A	312.95	2.0752	2.4528	1.18	2.6398	3.0338	1.15	2.9580	3.3357	1.13	3.1311	3.4923	1.12	3.2518	3.6121	1.11	3.3395	3.7171	1.11
Y	367.04	2.2273	2.7017	1.21	3.1212	3.6904	1.18	3.7470	4.2925	1.15	4.2450	4.7431	1.12	4.6121	5.0623	1.10	4.8343	5.3086	1.10
10X	473.56	2.7071	3.1340	1.16	3.5025	4.0243	1.15	3.9951	4.5406	1.14	4.3581	4.8799	1.12	4.5824	5.1228	1.12	4.8087	5.3542	1.11
Pd-4A	27.87	0.1582	0.1865	1.18	0.2349	0.2678	1.14	0.2837	0.3131	1.10	0.3131	0.3409	1.09	0.3322	0.3585	1.08	0.3474	0.3769	1.08
ZSM-5	272.30	1.7619	2.0009	1.14	2.2833	2.5310	1.11	2.5571	2.8202	1.10	2.7560	3.019	1.10	2.8941	3.1655	1.09	2.9917	3.2548	1.09
13X	97.93	0.5976	0.7020	1.17	0.7799	0.8942	1.15	0.8896	0.984	1.11	0.9706	1.065	1.10	1.0304	1.1213	1.09	1.0925	1.1720	1.07
CMS	340.35	2.4385	2.8545	1.17	3.3226	3.7167	1.12	3.8312	4.1814	1.09	4.1114	4.4644	1.09	4.2542	4.6235	1.09	4.3835	4.7338	1.08
VP800-5	360.34	2.3969	2.7800	1.16	3.0452	3.3708	1.11	3.3708	3.6773	1.09	3.6036	3.891	1.08	2.9193	3.3555	1.15	3.8792	4.1857	1.08
CMK-3	972.10	2.1338	2.9060	1.34	3.0392	3.7981	1.25	3.5974	4.3326	1.20	3.9860	4.6737	1.17	4.3120	4.9542	1.15	4.588	5.1809	1.13
SBA-15	653.29	1.4877	1.8517	1.24	2.1356	2.5516	1.19	2.5649	2.9635	1.16	2.8235	3.2048	1.14	3.0035	3.4021	1.13	3.1941	3.5754	1.12
SBA-15a	507.04	1.0404	1.2863	1.23	1.5482	1.8504	1.20	1.8908	2.1845	1.16	2.1245	2.4376	1.15	2.3223	2.6298	1.13	2.4939	2.8043	1.12
SBA-15b	489.38	0.9473	1.1115	1.17	1.3649	1.5729	1.15	1.6579	1.8878	1.14	1.8752	2.1269	1.13	2.0613	2.3115	1.12	2.2229	2.4747	1.11
SBA-15c	443.78	0.8168	0.9919	1.21	1.1923	1.4331	1.20	1.4618	1.7354	1.19	1.7009	1.9745	1.16	1.8838	2.1617	1.15	2.0259	2.3105	1.14
SBA-15d	431.36	0.7106	0.8291	1.17	1.0607	1.2158	1.15	1.3133	1.4775	1.13	1.5322	1.6782	1.10	1.6841	1.8356	1.09	1.8241	1.9700	1.08

BET surface area of adsorbents for  $\text{H}_2$  and  $\text{D}_2$ . The results indicate that good linear dependences are observed between the adsorption amount and the BET surface area at different pressures on microporous or mesoporous adsorbents; however, the slopes of the linearity are remarkably different between the microporous sections and the mesoporous sections. The linear correlation between the adsorption capacity and the BET surface area at the pressure of (0.04, 0.08, and 0.10) MPa are also coincident with the three pressures above according to the data in Table 1. The adsorption amount of adsorbents made of different materials located on a linear plot indicates that hydrogen isotope adsorption can only be monolayer coverage on adsorbent surfaces, and the difference in the interaction between the hydrogen isotope molecules and the solid surface

is not important for the adsorption capacity.<sup>4,5</sup> However, the specific surface area of adsorbents is a key factor for hydrogen isotope storage with the physical adsorption method. Moreover, pore size is more important than the surface properties of adsorbents for the adsorption amount of hydrogen isotopes, because the adsorption capacity on mesoporous molecular sieves is smaller than that on microporous molecular sieves at the same temperature, pressure, and BET surface area, which also explains the two sections for the two classes of adsorbents in Figures 10 to 12. It is well-known that the adsorption potential of the opposite walls is overlapped and the adsorption of hydrogen isotopes in micropores are thus enhanced,<sup>19</sup> but such overlap of adsorption potential does not occur in mesopores and, therefore, yields smaller adsorption capacity for the hydrogen

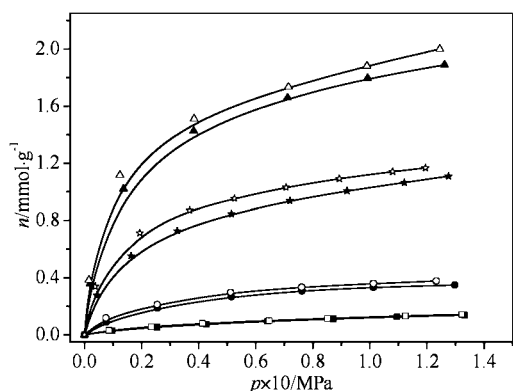


**Figure 5.** Adsorption isotherms of hydrogen and deuterium on different microporous adsorbents.  $\Delta$ ,  $\blacktriangle$ : 13X;  $\star$ ,  $\blackstar$ : 4A;  $\circ$ ,  $\bullet$ : Pd-4A;  $\square$ ,  $\blacksquare$ : 3A; hollow mark:  $\text{D}_2$ ; solid mark:  $\text{H}_2$ .

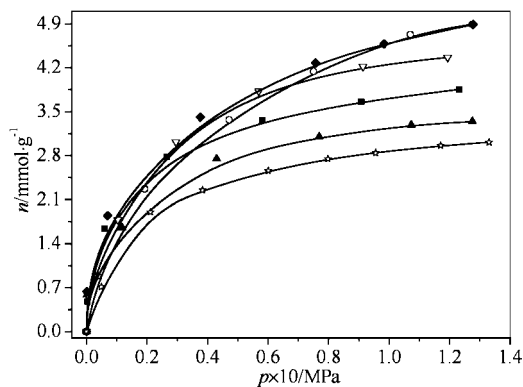


**Figure 6.** Adsorption isotherms of hydrogen on different microporous adsorbents.  $\blacksquare$ , VP800-5;  $\circ$ , Y;  $\blacktriangle$ , 5A;  $\nabla$ , CMS;  $\blacklozenge$ , 10X;  $\star$ , ZSM-5.

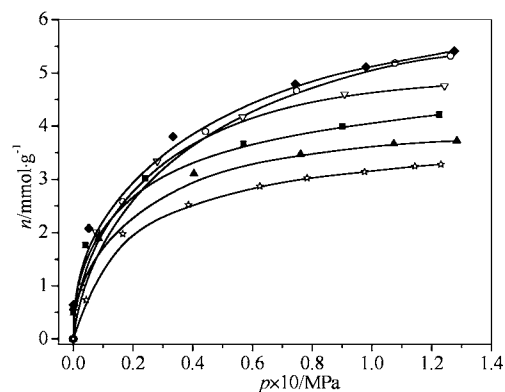


**Figure 7.** Adsorption isotherms of deuterium on different microporous adsorbents.  $\blacksquare$ , VP800-5;  $\circ$ , Y;  $\blacktriangle$ , 5A;  $\nabla$ , CMS;  $\blacklozenge$ , 10X;  $\star$ , ZSM-5.

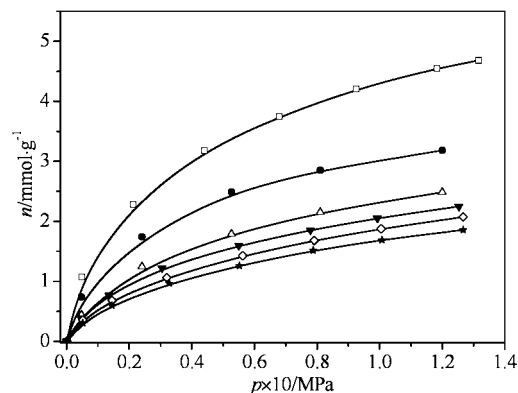


**Figure 8.** Adsorption isotherms of  $\text{H}_2$  on different mesoporous molecular sieves:  $\square$ , CMK-3;  $\bullet$ , SBA-15;  $\Delta$ , SBA-15 (a);  $\nabla$ , SBA-15 (b);  $\diamond$ , SBA-15 (c);  $\star$ , SBA-15 (d).

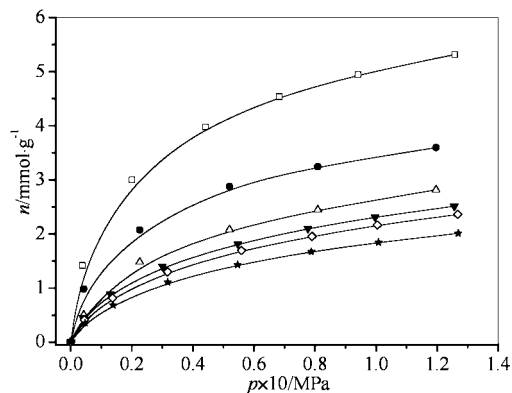


**Figure 9.** Adsorption isotherms of  $D_2$  on different mesoporous molecular sieves:  $\square$ , CMK-3;  $\bullet$ , SBA-15;  $\triangle$ , SBA-15 (a);  $\blacktriangledown$ , SBA-15 (b);  $\diamond$ , SBA-15 (c);  $\star$ , SBA-15 (d).

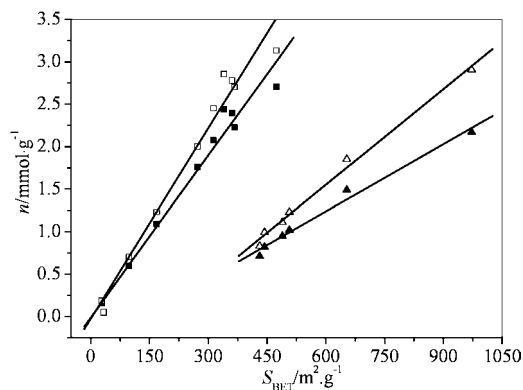


**Figure 10.** Dependence of the amount adsorbed on the specific surface area of different adsorbents at 0.02 MPa.  $\square$ ,  $\blacksquare$ : microporous;  $\triangle$ ,  $\blacktriangle$ : mesoporous.

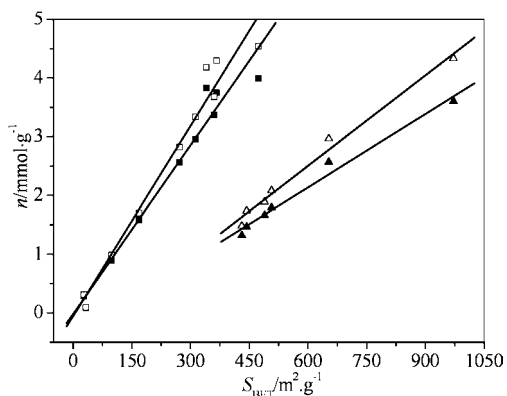


**Figure 11.** Dependence of the amount adsorbed on the specific surface area of different adsorbents at 0.06 MPa.  $\square$ ,  $\blacksquare$ : microporous;  $\triangle$ ,  $\blacktriangle$ : mesoporous.

isotopes. These observations are of great importance for how to select storage carriers of hydrogen isotope gas, namely, the material with a high specific surface area and microporous structure is the synthesis goal.

## Conclusion

The equilibrium adsorption amounts of hydrogen isotopes on different molecular sieves at 77 K and the BET surface area of molecular sieves were collected using a volumetric method. Good linear relationships were observed between the amount adsorbed and the BET surface area at different pressures on microporous or mesoporous molecular sieves, which provided proof of the monolayer adsorption mechanism for hydrogen

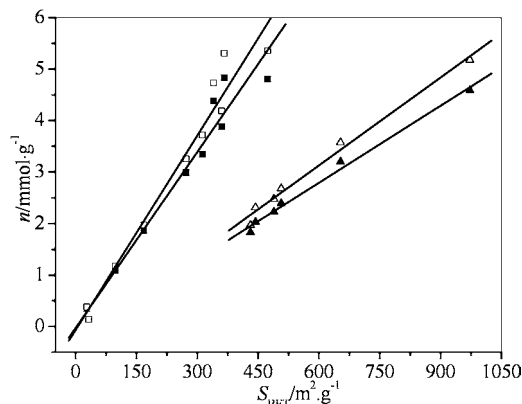


**Figure 12.** Dependence of the amount adsorbed on the specific surface area of different adsorbents at 0.12 MPa.  $\square$ ,  $\blacksquare$ : microporous;  $\triangle$ ,  $\blacktriangle$ : mesoporous.

isotope gas at supercritical temperatures. The adsorption capacity on mesoporous molecular sieves is smaller than that on microporous molecular sieves at the same temperature, pressure, and BET surface area. The adsorbent with the high specific surface area and microporous structure should be prepared for hydrogen isotope gas storage. The equilibrium adsorption difference between hydrogen and deuterium is increased with a decrease of pressure, and heavier hydrogen isotope molecules are preferentially adsorbed on these adsorbents. These results are of great significance to hydrogen isotope gas storage and PSA separation.

## Literature Cited

- (1) Zhou, L.; Zhou, Y. P.; Sun, Y. Studies on the mechanism and capacity of hydrogen uptake by physisorption-based materials. *Int. J. Hydrogen Energy* **2006**, *31*, 259–264.
- (2) Zhou, L.; Zhou, Y. P.; Sun, Y. A comparative study of hydrogen adsorption on superactivated carbon versus carbon nanotubes. *Int. J. Hydrogen Energy* **2004**, *29*, 475–479.
- (3) Zhou, L. Progress and problems in hydrogen storage methods. *Renewable Sustainable Energy Rev.* **2005**, *9*, 395–408.
- (4) Nijkamp, M. G.; Raaymakers, J. E. M. J.; van Dillen, A. J.; de Jong, K. P. Hydrogen storage using physisorption-materials demands. *Appl. Phys. A: Mater. Sci. Process.* **2001**, *72*, 619–623.
- (5) Ströbel, R.; Jörissen, L.; Schliermann, T.; Trapp, V.; Schütz, W.; Bohmhammel, K.; Wolf, G.; Gärche, J. Hydrogen adsorption on carbon materials. *J. Power Sources* **1999**, *84*, 221–224.
- (6) Liu, X. W.; Li, J. W.; Zhou, L.; Huang, D. S.; Zhou, Y. P. Mesoporous silica adsorbents synthesis, characterization, and their adsorption equilibrium properties for  $CO_2$ ,  $N_2$  and  $CH_4$ . *Chem. Phys. Lett.* **2005**, *415*, 198–201.
- (7) Chu, X. Z.; Zhou, Y. P.; Zhang, Y. Z.; Su, W.; Sun, Y.; Zhou, L. Adsorption of hydrogen isotopes on micro- and mesoporous adsorbents with orderly structure. *J. Phys. Chem. B* **2006**, *110*, 22596–22600.
- (8) Liu, X. W.; Zhou, L.; Li, J. W.; Sun, Y.; Su, W.; Zhou, Y. P. Methane sorption on ordered mesoporous carbon in the presence of water. *Carbon* **2006**, *44*, 1386–1392.
- (9) Zhu, Y. X.; Pan, X. M.; Xie, Y. C. Dispersion of sucrose on the surface of alumina. *Acta Phys. Chim. Sin.* **1999**, *15*, 830–833.
- (10) Chu, X. Z.; Zhao, Y. J.; Kan, Y. H.; Zhang, W. G.; Zhou, S. Y.; Zhou, Y. P.; Zhou, L. Dynamic experiments and model of hydrogen and deuterium separation with micropore molecular sieve Y at 77 K. *Chem. Eng. J.* **2009**, *152*, 428–433.
- (11) Gregg, S. J.; Sing, K. S. W. *Adsorption surface area and porosity*, 2nd ed.; St Edmundsbury Press: Suffolk, U.K., 1982.
- (12) Rouquerol, F.; Rouquerol, J.; Sing, K. *Adsorption by powders and porous solids*; Academic Press: London, 1999.
- (13) Sing, K. S. W. Adsorption methods for the characterization of porous materials. *J. Colloid Interface Sci.* **1998**, *76–77*, 3–11.
- (14) Sing, K. The use of nitrogen adsorption for the characterization of porous materials. *Colloid Surf., A* **2001**, *187–188*, 3–9.
- (15) Rouquerol, F.; Rouquerol, J.; Sing, K. *Adsorption by powders and porous solids: principles, methodology and applications*; Academic Press: London, 1999.

- (16) Do, D. D. *Adsorption analysis: equilibria and kinetics*; Imperial College Press: London, 1998.
- (17) Dai, W.; Zhou, Y. P.; Li, S. N.; Li, W.; Su, W.; Sun, Y.; Zhou, L. Thiophene capture with complex adsorbent SBA-15/Cu(I). *Ind. Eng. Chem. Res.* **2006**, *45*, 7892–7896.
- (18) Ruthven, D. M.; Farooq, S.; Knaebel, K. S. *Pressure Swing Adsorption*; VCH Publishers: New York, 1994.
- (19) Rzepka, M.; Lamp, P.; de la Casa-Lillo, M. A. Physisorption of hydrogen on microporous carbon and carbon nanotubes. *J. Phys. Chem. B* **1998**, *102*, 10894–10898.

Received for review October 25, 2009. Accepted January 7, 2010. The authors are grateful for the financial support of the Natural Science Foundation of Jiangsu Universities (08KJD530002, 09KJA530001), the financial support of the doctoral fund of Huaiyin Normal University, the financial support of Jiangsu Key Laboratory for Chemistry of Low-Dimensional Materials (JSKC09071), and the Program for Science and Technology Development of Huai'an (HAG09054-4).

JE9008798